SI-HEP-2013-18, QFET-2013-14, TTK-14-05, SFB/CPP-14-07, TUM-HEP-928/14

B-Meson Light-Cone Distribution Amplitude: Perturbative Constraints and Asymptotic Behaviour in Dual Space

Thorsten Feldmann* and Björn O. Lange†
Theoretische Elementarteilchenphysik, Universität Siegen, 57068 Siegen, Germany

Yu-Ming Wang‡
Institut für Theoretische Physik E, RWTH Aachen, 52056 Aachen, Germany;
Technische Universität München, Physik Department, 85747 Garching, Germany

(Dated: **4. April 2014)**

Based on the dual representation in terms of the recently established eigenfunctions of the evolution kernel in heavy-quark effective theory, we investigate the description of the B-meson light-cone distribution amplitude (LCDA) beyond tree-level. In particular, in dual space, small and large momenta do not mix under renormalization, and therefore perturbative constraints from a short-distance expansion in the parton picture can be implemented independently from non-perturbative modelling of long-distance effects. It also allows to (locally) resum perturbative logarithms from large dual momenta at fixed values of the renormalization scale. We construct a generic procedure to combine perturbative and non-perturbative information on the B-meson LCDA and compare different model functions and the resulting logarithmic moments which are the relevant hadronic parameters in QCD factorization theorems for exclusive B-meson decays.

PACS numbers: 12.38.Cy, 12.39.Hg, 13.25.Hw
Keywords: Heavy Quark Effective Theory, Light-Cone Expansion, Strong Interactions

arXiv:1404.1343v2 [hep-ph] 11 Apr 2014

I. INTRODUCTION

In a recent paper [1], it has been shown that the evolution kernel [2], which determines the 1-loop renormalization-group (RG) evolution of the B-meson light-cone distribution amplitude (LCDA) in heavy-quark effective theory (HQET), can be diagonalized by an appropriate integral transform. As the so-defined new function (dubbed "spectral" or "dual" in [1]) renormalizes *locally* with respect to its argument (denoted as ω' in the following), the properties at large and small values of ω' are clearly separated. In particular, we expect that for values of ω' much larger than the typical hadronic scale the dual function can be constrained by perturbative physics related to the operator product expansion (OPE) in the heavy-quark limit [3]. On the other hand, the behaviour at small values of ω' could be adjusted to results from non-perturbative QCD methods. Finally, the experimental results for exclusive B-decay observables constrain the logarithmic moments of the dual LCDA in QCD factorization theorems (see [4] and related work). In this way, one can construct parametrizations for the B-meson LCDA which include constraints from short- and long-distance theoretical predictions and experimental information simultaneously (for similar ideas in a different context see also [5] or [6]).

Our paper is organized as follows. In Sec. II we review the diagonalization of the renormalization kernel for the LCDA, which allows to describe the perturbative and non-perturbative domains of the dual function separately. In Sec. III we discuss the perturbative information available from regularized moments of the LCDA and translate them to the dual function. The main topic of this paper, to wit the construction of the dual LCDA from a given model ansatz while respecting all known perturbative constraints, is addressed in Sec. IV, and particularly in Eq. (24) below. In Sec. V we discuss the logarithmic moments of the dual function, with particular focus on the contributions from small and large values of ω'. Illustrative examples and their logarithmic moments are discussed in Sec. VI, followed by a summary and an appendix with mathematical details.

II. DIAGONALIZATION OF THE KERNEL

The leading LCDA of the B-meson in HQET, which is denoted as $\phi_B^+(\omega)$ in this work, is defined from the matrix element of a 2-particle light-cone operator [7],

$$\tilde{f}_B m_B\, \phi_B^+(\omega) = \int \frac{d\tau}{2\pi}\, e^{i\omega\tau} \times \langle 0|\bar{q}(\tau n)\,[\tau n,0]\,\not{n}\gamma_5\, h_v(0)|\bar{B}(m_B v)\rangle \qquad (1)$$

where n^μ is a light-like vector, $[\tau n,0]$ is a gauge-link represented by a Wilson line in the n^μ-direction, and $\tilde{f}_B$ is the B-meson decay constant in HQET. The variable ω represents the n-projection of the light quark's momentum.

The renormalization of the non-local light-cone operator in the presence of a static heavy quark in HQET induces a particular renormalization-scale dependence.

*Electronic address: thorsten.feldmann@uni-siegen.de
†Electronic address: lange@tp1.physik.uni-siegen.de
‡Electronic address: yuming.wang@tum.de

This gives rise to the Lange-Neubert (LN) kernel entering the renormalization-group equation (RGE) [2]

$$\frac{d}{d\ln\mu}\,\phi_B^+(\omega) \;=\; -\left[\Gamma_{\rm cusp}\,\ln\frac{\mu}{\omega}+\gamma_+\right]\phi_B^+(\omega) - \omega\int_0^\infty d\eta\,\Gamma(\omega,\eta)\,\phi_B^+(\eta)\,. \qquad (2)$$

The leading terms in the various contributions to the anomalous dimension in units of $\frac{\alpha_s}{4\pi}$ are

$$\Gamma^{(0)}_{\rm cusp}\equiv\Gamma_0=4\,C_F\,,\qquad \gamma_+^{(0)}\equiv\gamma_0=-2\,C_F\,,$$
$$\Gamma^{(0)}(\omega,\eta)=-\Gamma_0\left[\frac{\theta(\eta-\omega)}{\eta(\eta-\omega)}+\frac{\theta(\omega-\eta)}{\omega(\omega-\eta)}\right]_+\,. \qquad (3)$$

As shown in [3], the explicit solution for $\phi_B^+(\omega,\mu)$ can be written in closed form as a convolution integral involving hypergeometric functions. (If not otherwise stated, in the following the renormalization-scale dependence is implicitly understood, i.e. $\phi_B^+(\omega)\to\phi_B^+(\omega,\mu)$ etc. Similarly, the anomalous dimensions have a perturbative expansion in the strong coupling, $\Gamma_{\rm cusp}=\Gamma_{\rm cusp}(\alpha_s(\mu))$ etc.)

In a recent article [1] some of us have shown that the solution of the RG equation simplifies when the LCDA is represented in a "dual" momentum space, defined via

$$\phi_B^+(\omega) \;=\; \int_0^\infty\frac{d\omega'}{\omega'}\,\sqrt{\frac{\omega}{\omega'}}\,J_1\left(2\sqrt{\frac{\omega}{\omega'}}\right)\rho_B^+(\omega')\,, \qquad (4)$$

where ρ_B^+ defines a spectral function in the dual variable ω', and $J_1(z)$ is a Bessel function. (A similar relation holds for the other 2-particle LCDA $\phi_B^-(\omega)$, see [1], which reproduces the corresponding RGE in the Wandzura-Wilczek approximation [8–10].) The inverse transformation analogously reads

$$\rho_B^+(\omega') \;=\; \int_0^\infty\frac{d\omega}{\omega}\,\sqrt{\frac{\omega}{\omega'}}\,J_1\left(2\sqrt{\frac{\omega}{\omega'}}\right)\phi_B^+(\omega)\,. \qquad (5)$$

The dual function $\rho_B^+(\omega')$ now obeys the simple RGE

$$\frac{d\rho_B^+(\omega')}{d\ln\mu} \;=\; -\left[\Gamma_{\rm cusp}\,\ln\frac{\mu}{\hat\omega'}+\gamma_+\right]\rho_B^+(\omega')\,, \qquad (6)$$

which is local in the dual momentum ω'. Here, for convenience, we have defined the abbreviation

$$\hat\omega'\equiv e^{-2\gamma_E}\,\omega'\qquad(\text{and also }\hat\mu=e^{2\gamma_E}\,\mu)\,.$$

As a consequence the dual function $\rho_B^+(\omega')$ is renormalized multiplicatively,

$$\rho_B^+(\omega',\mu) \;=\; e^V\left(\frac{\mu_0}{\hat\omega'}\right)^{-g}\rho_B^+(\omega',\mu_0) \;\equiv\; U_{\omega'}(\mu,\mu_0)\,\rho_B^+(\omega',\mu_0)\,. \qquad (7)$$

The RG functions $V=V(\mu,\mu_0)$ and $g=g(\mu,\mu_0)$ are expressed in terms of the anomalous dimensions in the evolution kernel [2]; explicit expressions and a discussion of the composition rule of the RG elements,

$$U_{\omega'}(\mu_2,\mu_1)\,U_{\omega'}(\mu_1,\mu_0)=U_{\omega'}(\mu_2,\mu_0)\,, \qquad (8)$$

can be found in the appendix.

The transformation (4) thus diagonalizes the LN-kernel, which can also be seen by explicitly calculating the right-hand side of (2) for the identified *continuous* set of eigenfunctions [24],

$$\phi_B(\omega)\;\to\;f_{\omega'}(\omega)\equiv\sqrt{\frac{\omega}{\omega'}}\,J_1\left(2\sqrt{\frac{\omega}{\omega'}}\right)\,. \qquad (9)$$

In particular, using the 1-loop expression for the kernel, the non-local term in (2) yields

$$-\omega\int_0^\infty d\eta\,\Gamma^{(1)}(\omega,\eta)\,f_{\omega'}(\eta)=-\Gamma^{(1)}_{\rm cusp}\,\ln\frac{\omega}{\hat\omega'}\,f_{\omega'}(\omega)\,, \qquad (10)$$

which indeed combines with the local terms to the same RGE for $f_{\omega'}(\eta)$ as for $\rho_B^+(\omega')$ in (6), and the eigenvalues for the $f_{\omega'}(\omega)$ are

$$\gamma_{\omega'}=-\left(\Gamma_{\rm cusp}\,\ln\frac{\mu}{\hat\omega'}+\gamma_+\right)\,. \qquad (11)$$

The function $\rho_B^+(\omega')$ in dual momentum space thus plays a similar role as the set of Gegenbauer coefficients for the LCDAs of light mesons [11, 12], and the eigenfunctions $f_{\omega'}(\omega)$ are the analogue of the Gegenbauer polynomials $C_n^{(3/2)}(2u-1)$ for the quark momentum fraction u in a light meson. Notice however, that $\gamma_{\omega'}$ in (11) takes positive and negative values, and therefore – unlike for the case of the pion LCDA – an asymptotic shape of the B-meson LCDA at (infinitely) large RG scales does not exist. Still, as we will discuss below, perturbation theory implies model-independent constraints on the behaviour of $\rho_B^+(\omega')$.

III. POSITIVE MOMENTS OF ϕ_B^+

Following [3], we define positive moments of the LCDA $\phi_B^+(\omega,\mu)$ with a cut-off $\Lambda_{\rm UV}$ as

$$M_n(\Lambda_{\rm UV}):=\int_0^{\Lambda_{\rm UV}}d\omega\,\omega^n\,\phi_B^+(\omega)\,. \qquad (12)$$

For large $\Lambda_{\rm UV}\gg\Lambda_{\rm QCD}$, the moments are dominated by large values of ω in the integrand, and therefore can be estimated from a perturbative calculation based on the *partonic* result for the LCDA. For the first two moments ($n=0,1$) one obtains the 1-loop expressions [3],

$$M_0(\Lambda_{\rm UV}) = 1 + \frac{\alpha_s C_F}{4\pi}\left(-2\,\ln^2\frac{\Lambda_{\rm UV}}{\mu} + 2\,\ln\frac{\Lambda_{\rm UV}}{\mu} - \frac{\pi^2}{12}\right) + \frac{16\,\bar\Lambda}{3\,\Lambda_{\rm UV}}\,\frac{\alpha_s C_F}{4\pi}\left(\ln\frac{\Lambda_{\rm UV}}{\mu} - 1\right) + \dots\,,$$
$$M_1(\Lambda_{\rm UV}) = \Lambda_{\rm UV}\,\frac{\alpha_s C_F}{4\pi}\left(-4\,\ln\frac{\Lambda_{\rm UV}}{\mu} + 6\right) + \frac{4\bar\Lambda}{3}\left[1 + \frac{\alpha_s C_F}{4\pi}\left(-2\,\ln^2\frac{\Lambda_{\rm UV}}{\mu} + 8\,\ln\frac{\Lambda_{\rm UV}}{\mu} - \frac{7}{4} - \frac{\pi^2}{12}\right)\right] + \dots\,, \quad (13)$$

where the HQET-parameter $\bar\Lambda = m_B - m_b$ is defined in the pole-mass scheme. Expressing the moments M_n in terms of the dual function ρ_B^+, using (4), we obtain

$$M_n(\Lambda_{\rm UV}) = \int_0^\infty \frac{d\omega'}{\omega'} \int_0^{\Lambda_{\rm UV}} d\omega\,\omega^n \sqrt{\frac{\omega}{\omega'}}\,J_1\left(2\sqrt{\frac{\omega}{\omega'}}\right)\rho_B^+(\omega')\,. \quad (14)$$

The ω-integration can be performed explicitly, and for the first two moments this yields

$$M_0(\Lambda_{\rm UV}) = \Lambda_{\rm UV}\int_0^\infty \frac{d\omega'}{\omega'}\,J_2\left(2\sqrt{\frac{\Lambda_{\rm UV}}{\omega'}}\right)\rho_B^+(\omega')\,,$$
$$M_1(\Lambda_{\rm UV}) = \frac{2\Lambda_{\rm UV}}{3}\,M_0 - \frac{\Lambda_{\rm UV}^2}{3}\int_0^\infty \frac{d\omega'}{\omega'}\,J_4\left(2\sqrt{\frac{\Lambda_{\rm UV}}{\omega'}}\right)\rho_B^+(\omega')\,. \quad (15)$$

A. Fixed-Order Matching

Using properties of the Bessel functions summarized in the appendix, we write the perturbative expansion for the dual function as follows,

$$\rho_B^+(\omega')_{\rm pert.} = C_0(L)\,\frac{1}{\bar\Lambda}\,J_2\left(2\sqrt{\frac{2\bar\Lambda}{\omega'}}\right) + \frac{4\,(C_0(L) - C_1(L))}{\bar\Lambda}\,J_4\left(2\sqrt{\frac{2\bar\Lambda}{\omega'}}\right) + \dots\,, \quad (16)$$

which reproduces the moments M_0 and M_1 up to further power corrections in $\bar\Lambda/\Lambda_{\rm UV}$. At large values of $\omega' \gg \bar\Lambda$, this can also be approximated by

$$\rho_B^+(\omega')_{\rm pert} \overset{\omega'\gg\bar\Lambda}{\simeq} C_0(L)\,\frac{1}{\omega'} - \frac{2}{3}\,C_1(L)\,\frac{\bar\Lambda}{(\omega')^2} + \dots \quad (17)$$

The coefficient functions at first order in the strong coupling are obtained as

$$C_0(L) = 1 + \frac{\alpha_s C_F}{4\pi}\left(-2L^2 + 2L - 2 - \frac{\pi^2}{12}\right) + \mathcal{O}(\alpha_s^2)\,,$$
$$C_1(L) = 1 + \frac{\alpha_s C_F}{4\pi}\left(-2L^2 + 2L + \frac{5}{4} - \frac{\pi^2}{12}\right) + \mathcal{O}(\alpha_s^2)\,, \quad (18)$$

where the perturbative coefficients depend on logarithms

$$L = \ln\frac{\mu}{\hat\omega'}\,.$$

We observe that at tree level ($C_0 = C_1 = 1$) the expression in (16) reduces to the free parton model [13] as discussed in [1],

$$\rho_B^+(\omega')_{\rm part.} = \frac{1}{\bar\Lambda}\,J_2\left(2\sqrt{\frac{2\bar\Lambda}{\omega'}}\right)\,. \quad (19)$$

B. (Local) RG Improvement

The logarithms L in (18) become large for values of ω' much smaller or larger than μ. As the coefficients C_n in (18) fulfill the same 1-loop RGE as the dual function ρ_B^+,

$$\frac{d}{d\ln\mu}\,C_i = \frac{\alpha_s C_F}{4\pi}\,(-4L + 2)\,C_i + \mathcal{O}(\alpha_s^2) = -\frac{\alpha_s C_F}{4\pi}\left(\Gamma_{\rm cusp}^{(1)}\,\ln\frac{\mu}{\hat\omega'} + \gamma_+^{(1)}\right)C_i + \mathcal{O}(\alpha_s^2)\,, \quad (20)$$

we may resum perturbative logarithms into the RG function $U_{\omega'}$ as long as ω' is sufficiently large. To this end, we define

$$\mu_{\omega'} = \mu_{\omega'}(\mu) := \sqrt{(k\,\hat\omega')^2 + \mu^2}\,, \quad (21)$$

with a numerical parameter k with default value 1, such that $\mu_{\omega'} \sim \hat\omega'$ for large values of ω', and $\mu_{\omega'} \sim \mu$ at small values of ω'. With this we obtain an RG-improved expression for $\rho_B^+(\omega')_{\rm pert}$,

$$\rho_B^+(\omega',\mu)_{\rm RG} = U_{\omega'}(\mu,\mu_{\omega'})\,\rho_B^+(\omega',\mu_{\omega'})_{\rm pert}\,, \quad (22)$$

which is valid for $\omega' \gtrsim \mu$. (Notice that the implicit μ-dependence from the auxiliary scale $\mu_{\omega'}$ cancels between the two factors in (22) up to higher-order corrections which will be numerically checked by varying the parameter k.) The RG-improved form (22) is compared to the

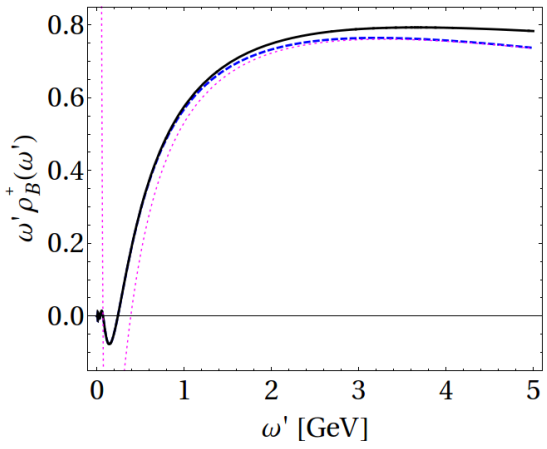

FIG. 1: Comparison of the perturbative expression for the dual function $\omega' \rho_B^+(\omega')$ at $\mu = 1$ GeV, with RG improvement (22, solid line) and without (16, dashed line). The dotted line shows the expansion for large ω' in (17). The HQET parameter $\bar{\Lambda}$ has been set to 465 MeV.

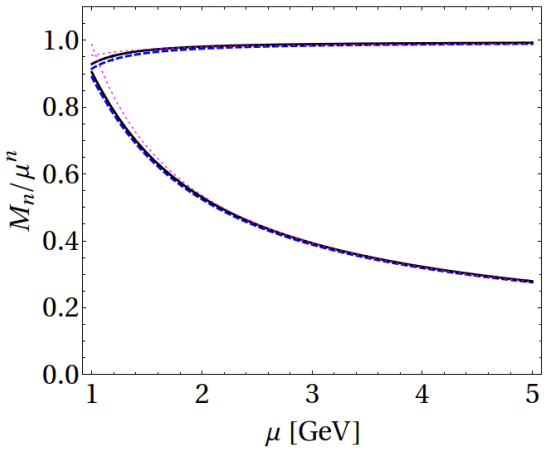

FIG. 2: Comparison of regularized moments $M_{0,1}$ as a function of μ with the UV cutoff set to $\Lambda_{\rm UV} = e^{\gamma_E}\,\mu$, computed from the perturbative expression for the dual function with RG improvement (22, solid lines) and without (16, dashed lines). The dotted line shows the result from the direct computation (13). Here M_0 evolves towards 1, while M_1/μ drops proportional to α_s. The HQET parameter $\bar{\Lambda}$ has been set to 465 MeV.

result from fixed-order perturbation theory (FOPT) in (16) in Fig. 1. As we discuss below, our new idea of local RG improvement is essential for the understanding of the asymptotic behaviour of ρ_B^+ for $\omega' \to \infty$. However, this resummation will only slightly modify the positive moments $M_{0,1}$ compared to the FOPT expressions in (13), as long as μ and $\Lambda_{\rm UV}$ are sufficiently large and of similar size. This is illustrated in Fig. 2.

For a given (high) scale $\mu \gg \bar{\Lambda}$ and large values of $\hat{\omega}' \gg \mu$, the dual function is thus completely determined perturbatively — independent of any hadronic model — with

$$\rho_B^+(\omega',\mu) \stackrel{\hat{\omega}' \gg \mu}{\longrightarrow} e^{V(\mu,\hat{\omega}')} \rho_B^+(\omega', \mu = \hat{\omega}')_{\rm pert.}\,. \tag{23}$$

IV. CONSTRUCTION OF $\rho_B^+(\omega')$

Our aim is now to find a systematic parametrization for the dual function $\rho_B^+(\omega',\mu)$ which interpolates between some low-energy model (valid at small renormalization scales and small values of ω') and the perturbative behaviour in (23), with the following features:

- Explicit implementation of the RG evolution as discussed above.
- Correct behaviour at large values of ω', such that the constraints on positive moments of $\phi_B^+(\omega,\mu)$ in HQET, as discussed above, are fulfilled.

Starting from a model function $\rho^{\rm model}(\omega')$, which is supposed to have a Taylor expansion in $1/\omega'$ at large values of ω' and to give a good description of the low-ω' region, we then propose the following ansatz

$$\begin{aligned}\rho_B^+(\omega',\mu) :=\;& U_{\omega'}\left(\mu,\mu_{\omega'}(\mu_0)\right)\left[\rho^{\rm model}(\omega') - \sum_{n=0}^{N} D_n^{\rm model}\, p_n(\omega')\right] \\ &+ U_{\omega'}\left(\mu,\mu_{\omega'}(\mu)\right) \sum_{n=0}^{N} D_n^{\rm pert}\left(\ln\frac{\mu_{\omega'}(\mu)}{\hat{\omega}'}, \mu_{\omega'}(\mu)\right) p_n(\omega')\,.\end{aligned} \tag{24}$$

In the first line we start with a given model $\rho^{\rm model}$ for the dual function and subtract a number of terms, with $\{p_n\}$ representing a set of appropriate functions which reduce to a power-law behaviour $1/(\omega')^{n+1}$ for large values of ω', and vanish quickly at small ω'. The term in square brackets then reduces to $\rho^{\rm model}$ for small values of ω' but now decreases as $1/(\omega')^{N+1}$ at large values of ω'. The evolution factor in front is chosen to refer to a hadronic reference scale μ_0 assigned to the input model [25]. The term in the second line uses the same set of basis functions to reproduce the RG-improved perturbative result in (22).

In the following analysis, we take the first two coefficients in that sum into account ($N = 1$). The coefficients D_n can then be matched by expanding the corresponding perturbative or model functions for large values of ω', which will be done below. For the set of functions p_n we choose

$$p_n(\omega') \equiv \frac{\Omega^n}{(\omega'+\Omega)^{n+1}}\, e^{-\Omega/\omega'}\,, \tag{25}$$

so that the modifications from the perturbative matching are exponentially suppressed at small values of ω', where the original model is supposed to give a reasonable functional description. The auxiliary parameter Ω sets the scale where the transition between the perturbative and non-perturbative regime occurs.

A. Models

The coefficients D_n can easily be extracted by comparing the Taylor expansion in $1/\omega'$. For instance, for the exponential model

$$\rho^{\rm model-1}(\omega') = \frac{1}{\omega'}\, e^{-\omega_0/\omega'}\,, \tag{26}$$

one obtains

$$D_0^{\rm model-1} = 1\,, \quad D_1^{\rm model-1} = 2 - \frac{\omega_0}{\Omega}\,. \tag{27}$$

and for the free parton model [13], as discussed in [1],

$$\rho^{\rm model-2}(\omega') = \frac{1}{\bar\Lambda}\, J_2\left(2\sqrt{\frac{2\bar\Lambda}{\omega'}}\right)\,, \tag{28}$$

one gets

$$D_0^{\rm model-2} = 1\,, \quad D_1^{\rm model-2} = 2 - \frac{2\bar\Lambda}{3\Omega}\,. \tag{29}$$

As a third illustrative model, we consider the tree-level estimate of a QCD sum-rule analysis in [14] where $\phi_B^+(\omega) = 3/4/\omega_0^3\,\theta(2\omega_0-\omega)\,\omega\,(2\omega_0-\omega)$ which corresponds to

$$\rho^{\rm model-3}(\omega') = \frac{3}{\omega_0}\,\sqrt{\frac{\omega'}{2\omega_0}}\, J_3\left(2\,\sqrt{\frac{2\omega_0}{\omega'}}\right)\,, \tag{30}$$

and

$$D_0^{\rm model-3} = 1\,, \quad D_1^{\rm model-3} = 2 - \frac{\omega_0}{2\Omega}\,. \tag{31}$$

B. Matching with OPE

The ansatz (24) reduces straight-forwardly to an expression in FOPT by setting $\mu_{\omega'}(\mu) = \mu_{\omega'}(\mu_0) = \mu$. The matching coefficients $D_n^{\rm pert}$ are then easily obtained by equating the resulting large-ω' expansion with (17). For the first two coefficients, we obtain

$$\begin{aligned} D_0^{\rm pert}\left(\ln\frac{\mu_{\omega'}}{\hat\omega'}, \mu_{\omega'}\right) &= C_0\left(\ln\frac{\mu_{\omega'}}{\hat\omega'}, \mu_{\omega'}\right)\,, \\ D_1^{\rm pert}\left(\ln\frac{\mu_{\omega'}}{\hat\omega'}, \mu_{\omega'}\right) &= 2C_0\left(\ln\frac{\mu_{\omega'}}{\hat\omega'}, \mu_{\omega'}\right) \\ &\quad - \frac{2\bar\Lambda}{3\Omega}\, C_1\left(\ln\frac{\mu_{\omega'}}{\hat\omega'}, \mu_{\omega'}\right)\,. \end{aligned} \tag{32}$$

Notice that, at this stage, the parameter Ω is arbitrary. However, as we will see in the numerical analysis, the dependence of the $\rho_B^+(\omega,\mu)$ on the value of Ω is not very pronounced. For concreteness, we will use a default value of $\Omega = e^{\gamma_E}\mu_0$.

V. LOGARITHMIC MOMENTS

The logarithmic moments of the dual function can be defined as

$$L_k(\mu) \equiv \int_0^\infty \frac{d\omega'}{\omega'}\, \ln^k\left(\frac{\hat\omega'}{\mu}\right) \rho_B^+(\omega',\mu)\,. \tag{33}$$

As emphasized in [1] the first three logarithmic moments ($k = 0, 1, 2$) of $\phi_B^+(\omega)$ are identical to those of $\rho_B^+(\omega')$. They represent the hadronic input parameters appearing in factorization theorems for exclusive B-meson decays to first non-trivial order in the strong coupling constant.

- Contributions from $\hat\omega' \geq \mu$ are completely determined perturbatively via (23),

  $$L_k^+(\mu) \equiv \int_\mu^\infty \frac{d\hat\omega'}{\hat\omega'}\, \ln^k\left(\frac{\hat\omega'}{\mu}\right) e^{V(\mu,\hat\omega')} \rho_B^+(\omega', \mu=\hat\omega')_{\rm pert.}\,. \tag{34}$$

  This will be illustrated and confirmed numerically in Sec. VI.

- For the contributions from $\hat\omega' \leq \mu$, substituting $z = -\ln\frac{\hat\omega'}{\mu}$,

  $$L_k^-(\mu) \equiv \int_0^\infty dz\,(-z)^k\, \rho_B^+(\hat\mu\, e^{-z}, \mu)\,, \tag{35}$$

  we may expand the function $\rho_B^+(\omega',\mu)$ in terms of Laguerre polynomials $\mathrm{L}_n(z)$,

  $$\rho_B^+(\hat\mu\, e^{-z}, \mu) := \sum_{n=0}^\infty a_n(\mu)\, e^{-z}\, \mathrm{L}_n(z)\,. \tag{36}$$

  For a given model, the coefficients $a_n(\mu)$ can be obtained from the orthogonality relation (A3). The logarithmic moments simply follow as

  $$\begin{aligned} L_0^-(\mu) &= a_0(\mu)\,, \\ L_1^-(\mu) &= a_1(\mu) - a_0(\mu)\,, \\ L_2^-(\mu) &= 2a_2(\mu) - 4a_1(\mu) + 2a_0(\mu)\,, \\ &\quad \text{etc.} \end{aligned} \tag{37}$$

In principle the first few L_k^- – and hence the first few a_k – can be determined from precision analyses of radiative leptonic B-meson decays (see [15, 16] for recent discussions). On the theory side the task is difficult. When more information on the perturbative analysis of the moments M_n becomes available, it only affects the precision of our knowledge of L_k^+, but does not spill over into the non-perturbative contribution. It may be interesting to see if non-perturbative methods like sum rules and lattice QCD are able to shed more light on the Laguerre coefficients in L_k^-, once the dual function ρ_B^+ is used in lieu of ϕ_B.

A. Large-Scale Behaviour

As we have seen, at tree-level in FOPT the dual function $\rho_B^+(\omega')$ behaves as $\sim 1/\omega'$ for large values of ω', see (17). This behaviour is softened by (global) evolution towards higher scales, i.e.

$$g = g(\mu,\mu_0) > 0 \qquad \text{for } \mu > \mu_0$$

in (7), which induces an additional factor $(\omega')^g$. Therefore it appears as if for sufficiently large values of g the ω'-integrals which, for instance, determine the transformation back to ω-space in (4) or the logarithmic moments in (33), would no longer converge. (In other words it seems as if ρ_B undergoes a qualitativ change by evolving to sufficiently large scales $\mu \gg \mu_0$ such that $g(\mu,\mu_0) \geq 1$.) The local RG improvement as it is implemented in (22) reveals, however, that the perturbative resummation of logarithms $\ln \omega'/\mu$ from the region $\omega' \gg \mu$ always yields converging results, since at large (but fixed) values of μ one rather has

$$\rho_B^+(\omega',\mu) \sim (\omega')^{-1-g(\mu_{\omega'},\mu)}$$

and $g(\mu_{\omega'},\mu) > 0$ for $\hat{\omega}' \gg \mu$. Therefore, in that asymptotic region, the function $\rho_B^+(\omega')$ always decreases *faster* than $1/\omega'$, which can also be seen from Fig. 3 where we compare the behaviour of $\rho_B^+(\omega')$ at different renormalization scales.

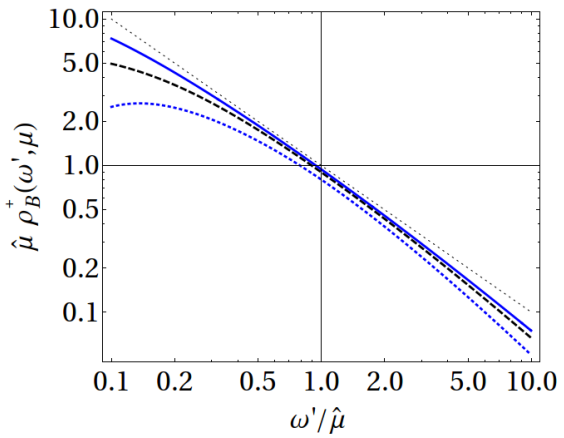

FIG. 3: Double logarithmic plot for the behaviour of $\hat{\mu}\,\rho_B^+(\omega',\mu)$ for model-1 at different renormalization scales, $\mu = 1$ GeV (thick dotted line), $\mu = 3$ GeV (dashed line), $\mu = 10$ GeV (solid line), compared to the naive asymptotic $\hat{\mu}/\omega'$ behaviour at large values of ω' (thin dotted line, which is the only one that truly goes through the point $(1,1)$).

For phenomenological applications in exclusive B-meson decays one always has $g(\mu,\mu_0) < 1$, but we may still formally consider the case $g \geq 1$ for curiosity. From the discussion in the previous paragraph, we conclude that the solution of the RGE for the dual function $\rho_B^+(\omega',\mu)$ makes sense for arbitrary values of μ and μ_0 (provided they are sufficiently larger than $\Lambda_{\rm QCD}$). In contrast, the derivation of the RGE solutions for the original LCDA in (1) – as discussed in [3, 13] – is formally restricted to values $0 < g(\mu,\mu_0) < 1$. So we repeat for clarity's sake that the logarithmic moments L_k exist at *all* scales $\mu \gg \Lambda_{\rm QCD}$, and that perceived thresholds are mathematical artifacts.

VI. NUMERICAL EXAMPLES

A. Preliminaries

Mass-renormalization and $\bar{\Lambda}$: For the numerical analysis, we take the b-quark mass from a determination in a different mass scheme, the shape-function (SF) scheme [17], which is related to the pole-mass scheme via

$$\bar{\Lambda} = \bar{\Lambda}_{\rm SF}(\mu_f,\mu) - \mu_f \,\frac{\alpha_s(\mu)\,C_F}{\pi}\left(1 - 2\,\ln\frac{\mu_f}{\mu}\right), \quad (38)$$

with a fixed reference scale $\mu_f \sim \mu$. The HFAG 2013 update [18] quotes

$$\bar{\Lambda}_{\rm SF}(\mu_*,\mu_*) = (0.691 \pm 0.025)\ \text{GeV}\,,$$

for a common value $\mu = \mu_f = \mu_* = 1.5$ GeV. For the numerical discussion in the pole-mass scheme [26], this corresponds to using

$$\bar{\Lambda} = (0.465 \pm 0.025)\ \text{GeV}\,.$$

Hadronic reference scale: As our default choice for a hadronic reference scale, we use

$$\mu_0 = 1.0\ \text{GeV}\,.$$

The dimensionless parameter k in (21) is taken at a default value $k = 1$ and varied between $k = 1/2$ and $k = 2$. As already mentioned above, our default choice for the scale-parameter Ω in the functions $p_n(\omega')$ is set to

$$\Omega = e^{\gamma_E}\,\mu_0 \simeq 1.78\ \text{GeV}\,.$$

Again this value will be varied within a factor of 2 to study the sensitivity of our parametrization with respect to this parameter.

Running coupling constant: For $\alpha_s(\mu)$ we take the 3-loop formula (B3) with a fixed number of flavours $n_f = 4$, and $\Lambda^{(4)}_{\rm QCD} \simeq 299$ MeV, which corresponds to

$$\alpha_s(1\ \text{GeV}) \simeq 0.466\,, \qquad \alpha_s(5\ \text{GeV}) \simeq 0.214\,.$$

We also take into account the 3-loop β-function in the evaluation of the RG function g (see appendix).

Model 1: The parameter ω_0 in (26) at $\mu = 1.0$ GeV is set to 438 MeV, where we have used the value advocated in [3].

Model 2: The free parton model does not involve additional hadronic parameters, except for the HQET parameter $\bar{\Lambda}$, together with the low-energy reference scale μ_0, which have already been fixed above.

Model 3: The tree-level sum rule estimate in [14] contains a parameter $\omega_0 = 1.0$ GeV at $\mu_0 = 1.0$ GeV.

B. Illustrations

ρ_B^+ at large values of ω': In Fig. 4, we present the result for the product $\omega' \rho_B^+(\omega, \mu)$ at large values $\omega' > \mu_0$ for two choices of renormalization scale, $\mu_0 = 1$ GeV and $\mu = 5$ GeV. We observe that the inclusion of the radiative corrections shows a significant effect compared to the original (tree-level) functions $\rho^{\rm model}(\omega')$, while the differences among the different models is irrelevant at large values of ω'.

ρ_B^+ at small values of ω': In Fig. 5, we present the results for $\rho_B^+(\omega, \mu)$ at small values $\omega' < \mu_0$ for two choices of renormalization scale, μ_0 and $\mu = 5$ GeV. We observe that for our default value of the parameter Ω the original model is reproduced extremely well, and the variation of this parameter has only a minor effect at intermediate values of ω'.

The LCDA $\phi_B^+(\omega)$: From the QCD-improved dual function $\rho_B^+(\omega', \mu)$ in (24) for a given input model, we can easily compute the corresponding LCDA $\phi_B^+(\omega, \mu)$ via (4) by numerical integration. We have compared the original (tree-level) models of $\phi_B^+(\omega, \mu_0)$ and their QCD-improved versions for the 3 benchmark models. For all three models we recovered the feature of a (negative) "radiative tail" at large values of ω [3], while the behaviour at small values of ω is practically unaffected.

Regularized moments of ϕ_B^+: In Table I we list the first two (regularized) moments M_0 and M_1 as obtained from different models and different renormalization scales, and compare them to the perturbative result obtained from the local RG-improved formula (22). Here, the value for the UV cutoff is chosen slightly larger than the renormalization scale, $\Lambda_{\rm UV} := e^{\gamma_E}\,\mu$, in order to assure that the result is sufficiently dominated by the radiative tail in the corresponding LCDA $\phi_B^+(\omega)$. We observe that the zeroth moment is reproduced rather accurately by the different models; the first moments differ more, around 10% at $\mu = 10$ GeV. These differences are easily explained by the fact that those higher-order terms in M_1 which are not fixed by the matching procedure are of the order $1/\alpha_s \cdot \Omega^2/\Lambda_{\rm UV}^2$ relative to M_1.

	μ	model-1	model-2	model-3	pert. (RG)
M_0	3 GeV	0.996	0.995	0.998	0.988
	6 GeV	1.032	1.024	1.036	0.993
	10 GeV	1.011	1.004	1.014	0.995
M_1/μ	3 GeV	0.454	0.383	0.494	0.393
	6 GeV	0.329	0.287	0.351	0.250
	10 GeV	0.207	0.183	0.219	0.188

TABLE I: Comparison between the regularized moments M_0 and M_1 from the QCD-improved model functions for ϕ_B^+ and the RG-improved perturbative results from (16,22) at different values of μ with $\Lambda_{\rm UV} = e^{\gamma_E}\,\mu$.

Logarithmic Moments: In Table II, we compare the numerical results for the first three logarithmic moments $L_{0,1,2}$ following from the three different benchmark models. In the upper part, we consider an intermediate scale $\mu = 3$ GeV and separate the contributions to the integral from regions where $\hat{\omega}'$ is smaller or larger than μ. We observe that the former – by construction –

L_n	total	from $\hat{\omega}' < \mu$	from $\hat{\omega}' \geq \mu$
L_0 (model 1)	1.67	1.58	0.086
L_0 (model 2)	1.65	1.57	0.086
L_0 (model 3)	1.21	1.12	0.086
L_1 (model 1)	-3.85	-3.93	0.074
L_1 (model 2)	-3.46	-3.54	0.074
L_1 (model 3)	-2.19	-2.27	0.074
L_2 (model 1)	11.6	11.4	0.121
L_2 (model 2)	9.03	8.91	0.121
L_2 (model 3)	5.44	5.32	0.121

L_n	total (RG)	FOPT	input (tree)
L_0 (model 1)	2.19	2.12	2.28
L_0 (model 2)	2.05	1.98	2.15
L_0 (model 3)	1.40	1.34	1.50
L_1 (model 1)	-3.31	-3.45	-3.20
L_1 (model 2)	-2.41	-2.56	-2.31
L_1 (model 3)	-1.31	-1.46	-1.21
L_2 (model 1)	7.88	7.19	8.25
L_2 (model 2)	4.25	3.56	4.62
L_2 (model 3)	2.48	1.80	2.85

TABLE II: Logarithmic moments L_n from different models (values in GeV^{-1}). The theoretical uncertainties are dominated by the hadronic input model. *Above:* Comparison between the contributions from low and high ω' regions at $\mu = 3$ GeV. *Below:* Effects of the perturbative and local RG improvement at $\mu_0 = 1$ GeV.

very much depend on the specific hadronic input model. The contributions to the moments from large values, $\hat{\omega}' > \mu$, on the other hand, are completely determined by perturbative matching and RG evolution and therefore independent of the hadronic input model, in line with the discussion around (23). In the lower half of the table, we illustrate the effects of the perturbative constraints by comparing the moments originating from the hadronic input function with its modifications from FOPT alone and its (locally) RG-improved version, at the hadronic input scale $\mu_0 = 1$ GeV. Again, we observe that the logarithmic moments before and after the perturbative improvement are highly correlated and do not differ very much.

VII. SUMMARY

The dual function $\rho_B^+(\omega')$ of the heavy B-meson, which plays a similar role to the familiar set of Gegenbauer coefficients for light-meson LCDAs, has been the subject of this paper. To recapitulate and summarize we have highlighted that the transformation between the LCDAs in momentum space, $\phi_B^+(\omega)$, and dual momentum space, $\rho_B^+(\omega')$, consists of eigenfunctions of the RG evolution kernel for $\phi_B^+(\omega)$. The dual function renormalizes multiplicatively, unlike the LCDA ϕ_B^+, which in particular implies that the non-perturbative low-ω' region does not mix with the perturbative domain, $\omega' \gtrsim \mu$.

We have demonstrated that the dual function in the perturbative domain is calculable from the OPE results of a finite-moment analysis of ϕ_B^+ [3], and determined its values in the region $\omega' \sim \mu$. By resumming perturbative logarithms we have shown that ρ_B vanishes faster than $1/\omega'$ for $\omega' \gg \mu$, such that its first inverse moment, $\lambda_B^{-1}(\mu)$, converges for $\omega' \to \infty$ at any perturbative scale μ. This result distinguishes the analysis of λ_B and related quantities in dual momentum space from the corresponding one using the standard LCDA ϕ_B^+, which appears to suffer from artificial thresholds in its RG evolution when the RG function $g(\mu, \mu_0)$ assumes positive integer values.

The low-ω' regime is not accessible via perturbation theory. It must be determined by other means, but can be modelled in the meantime. We have developed a method of combining a model ansatz in the non-perturbative regime with the perturbative results that respects the moment constraints and smoothly connects both domains. This was achieved by correcting the first few terms in the large-ω' behaviour of the model, which is shown in Eq. (24). The keen-eyed reader might inquire whether taking ever more terms into account in this manner will ultimately determine the dual function and thus render the modelled part superfluous. We found only poor or no convergence with such an approach, depending on the choice of basis functions p_n, which points towards an unrelatedness between λ_B and other HQET parameters like $\bar{\Lambda}$ within perturbative methods.

We have illustrated our results using three different models, and also performed a numerical analysis for the phenomenologically relevant logarithmic moments L_k. Following the gist of our discussion thus far, we split $L_k = L_k^+ + L_k^-$ between the regions $\hat{\omega}' > \mu$ and $\hat{\omega}' < \mu$. While the contributions L_k^+ are model-independent (and small), the hadronic model dominates the moments. In principle the L_k^- can be determined from precision analyses of radiative leptonic B-meson decays, but this only determines the first few terms in an expansion of the dual function in terms of Laguerre polynomials in the variable $z = \ln \mu/\hat{\omega}'$ for $\hat{\omega}' \leq \mu$.

The perturbative analysis of the B-meson LCDA is restricted to 1-loop accuracy so far. From the theoretical perspective, it would be interesting to see to what extent the picture that emerged from our analyses continues to be valid when implementing 2-loop corrections to the evolution kernel and the perturbative moment constraints, together with higher power corrections in HQET.

Acknowledgments

TF and BOL acknowledge support by the Deutsche Forschungsgemeinschaft (DFG) within the Research Unit FOR 1873 (*Quark Flavour Physics and Effective Field Theories*). YMW is supported by the *DFG-Sonderforschungsbereich/Transregio 9 "Computergestützte Theoretische Teilchenphysik"*. We are particularly grateful to Guido Bell who continually accompanied the project and contributed many valuable discussions and comments and critical reading of the manuscript. TF also would like to thank Thomas Mannel for helpful discussions.

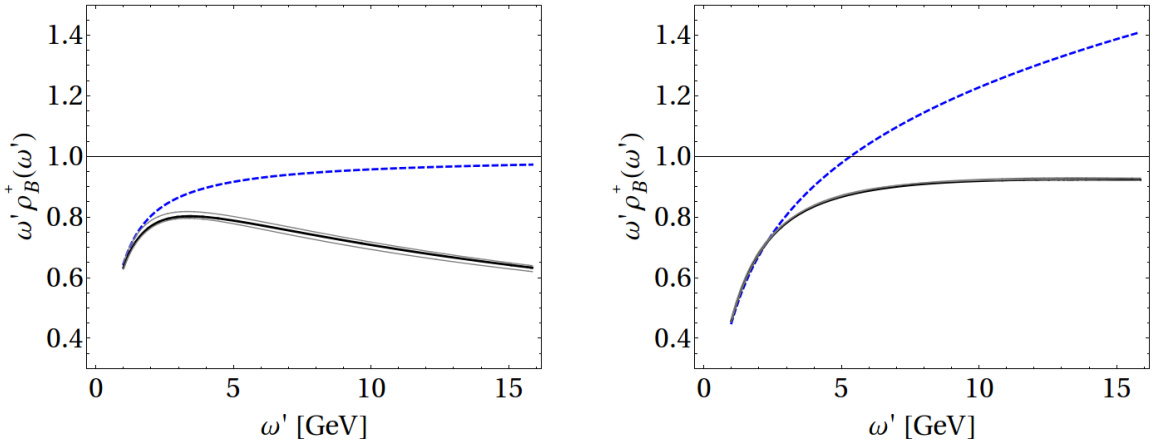

FIG. 4: Behaviour of the dual function $\rho_B^+(\omega')$ (multiplied with a factor ω') at large values of ω'. We show the result for model-1; for models-2,3 the result looks almost identical. Left: For $\mu = \mu_0$. Right: For $\mu = 5$ GeV. The solid lines represent the result of the RG-improved parametrization (24). The grey lines indicate the variation of the parameter $k = 1/2, 2$ in the defintion of the auxiliary scale $\mu_{\omega'}$. The thick (blue) dashed lines refer to the original model function $\rho^{\text{model}-1}(\omega')$. (Notice that in the right plot, the model function is [globally] evolved from $\mu_0 \to 5$ GeV.)

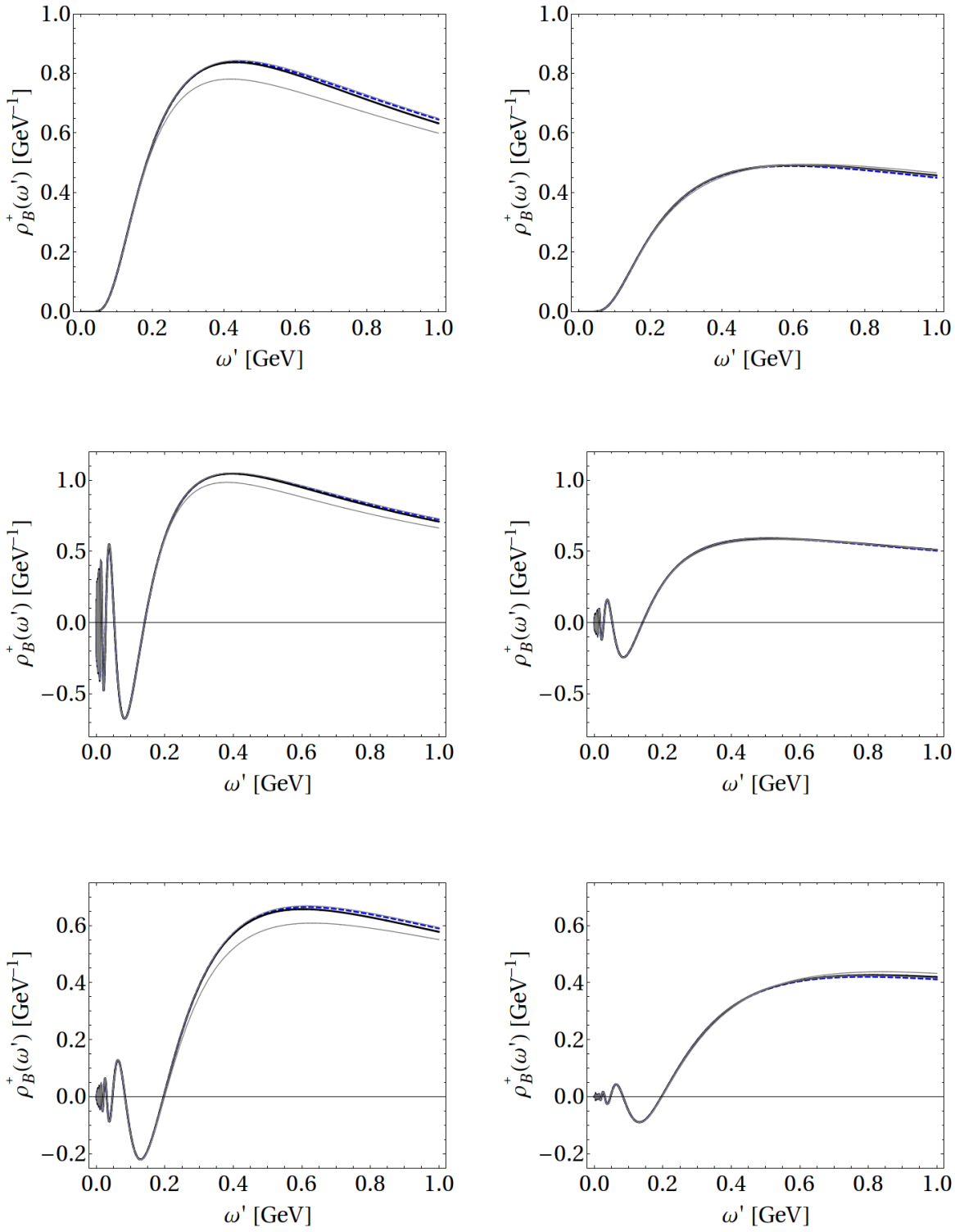

FIG. 5: Behaviour of the dual function $\rho_B^+(\omega')$ at small values of ω'. From top to bottom we show model-1, 2, 3. Left: For $\mu = \mu_0$. Right: For $\mu = 5$ GeV. The solid line represents the result of the RG-improved parametrization (24). The grey lines indicate the variation of the parameter Ω, appearing in the functions $p_n(\omega')$, within a factor of two. The thick (blue) dashed line refers to the original model functions $\rho^{\text{model}-1,2,3}(\omega')$. (Notice that in the right plots, the model functions are evolved from $\mu_0 \to 5$ GeV.)

Appendix A: Some Properties of Special Functions

We use the completeness relation for Bessel functions in the form

$$\int_0^\infty \frac{d\omega'}{\omega'}\,\frac{1}{\omega'}\,J_n\left(2\sqrt{\frac{a}{\omega'}}\right)J_n\left(2\sqrt{\frac{b}{\omega'}}\right)=\int_0^\infty d\omega\,J_n\left(2\sqrt{a\omega}\right)J_n\left(2\sqrt{b\omega}\right)=\delta(a-b)\,. \tag{A1}$$

Among others, this allows to revert the relation between the regularized moments $M_{0,1}$ and the dual function $\rho_B^+(\omega',\mu)$ for large values of $\hat{\omega}'\sim\mu$

$$\rho_B^+(\omega')=\frac{1}{\omega'}\int_0^\infty\frac{d\Lambda_{\rm UV}}{\Lambda_{\rm UV}}\left\{M_0\Big|_{\bar\Lambda\to0}\times J_2\left(2\sqrt{\frac{\Lambda_{\rm UV}}{\omega'}}\right)+\frac{\partial}{\partial\bar\Lambda}\left(2M_0-\frac{3M_1}{\Lambda_{\rm UV}}\right)_{\bar\Lambda\to0}\times\bar\Lambda\,J_4\left(2\sqrt{\frac{\Lambda_{\rm UV}}{\omega'}}\right)+\dots\right\}. \tag{A2}$$

The Laguerre polynomials satisfy the orthogonality relation

$$\int_0^\infty dz\,e^{-z}\,{\rm L}_n(z)\,{\rm L}_m(z)=\delta_{nm}\,. \tag{A3}$$

The explicit expressions for $n=0,1,2$ read

$$L_0(z)=1\,,\qquad L_1(z)=1-z\,,\qquad L_2(z)=\frac{1}{2}\left(z^2-4z+2\right)\,. \tag{A4}$$

Appendix B: Explicit Form of RG Functions

The expansions of the QCD β-function and the anomalous dimensions in the LN kernel are defined as

$$\beta=-8\pi\left(\beta_0\left(\frac{\alpha_s}{4\pi}\right)^2+\beta_1\left(\frac{\alpha_s}{4\pi}\right)^3+\beta_2\left(\frac{\alpha_s}{4\pi}\right)^4+\dots\right)\,, \tag{B1}$$

with

$$\begin{aligned}&\beta_0=\frac{11}{3}\,C_A-\frac{2}{3}\,n_f\,,\quad \beta_1=\frac{34}{3}\,C_A^2-\frac{10}{3}\,C_An_f-2\,C_Fn_f\,,\\ &\beta_2=\frac{2857}{54}\,C_A^3+\left(C_F^2-\frac{205}{18}\,C_FC_A-\frac{1415}{54}\,C_A^2\right)n_f+\left(\frac{11}{9}\,C_F+\frac{79}{54}\,C_A\right)n_f^2\,.\end{aligned} \tag{B2}$$

With this we express the 3-loop running coupling constant as

$$\alpha_s(\mu)=\frac{2\pi}{\beta_0L}\left(1-\frac{\beta_1\ln(2L)}{2\beta_0^2L}+\frac{\beta_1^2\left(\frac{\beta_0\beta_2}{\beta_1^2}+\left(\ln(2L)-\frac{1}{2}\right)^2-\frac{5}{4}\right)}{4\beta_0^4L^2}\right)\,,\qquad L=\ln\frac{\mu}{\Lambda_{\rm QCD}^{(n_f)}}\,. \tag{B3}$$

For the considered range of RG scales, we take $n_f=4$ with $\Lambda_{\rm QCD}^{(4)}=299$ MeV.
The first coefficient of the anomalous dimension,

$$\gamma_+=\frac{\alpha_s}{4\pi}\,\gamma_0+\dots\,, \tag{B4}$$

reads $\gamma_0=-2\,C_F$ [2].
The coefficients in the perturbative expansion of the cusp anomalous dimension,

$$\Gamma_{\rm cusp}=\frac{\alpha_s}{4\pi}\,\Gamma_0+\left(\frac{\alpha_s}{4\pi}\right)^2\Gamma_1+\left(\frac{\alpha_s}{4\pi}\right)^3\Gamma_2+\dots\,, \tag{B5}$$

read [19–21]

$$\begin{aligned}&\Gamma_0=4\,C_F\,,\quad \Gamma_1=C_F\left(\left(\frac{268}{9}-\frac{4\pi^2}{3}\right)C_A-\frac{40}{9}\,n_f\right)\,,\\ &\Gamma_2=16C_F\left(\left(-\frac{7\zeta(3)}{3}-\frac{209}{108}+\frac{5\pi^2}{27}\right)C_An_f+\left(\frac{11\zeta(3)}{6}+\frac{245}{24}-\frac{67\pi^2}{54}+\frac{11\pi^4}{180}\right)C_A^2+\left(2\zeta(3)-\frac{55}{24}\right)C_Fn_f-\frac{n_f^2}{27}\right)\,.\end{aligned} \tag{B6}$$

The RG elements $U_{\omega'}(\mu,\mu_0)$ have been defined in (7) as

$$U_{\omega'}(\mu,\mu_0) = \exp\left[V(\mu,\mu_0) - g(\mu,\mu_0)\,\ln\frac{\mu_0}{\hat{\omega}'}\right], \tag{B7}$$

with the RG functions g and V defined as (see e.g. [22])

$$g(\mu,\mu_0) = \int_{\alpha_s(\mu_0)}^{\alpha_s(\mu)} \frac{d\alpha}{\beta(\alpha)}\,\Gamma_{\rm cusp}(\alpha)\,, \qquad V(\mu,\mu_0) = -\int_{\alpha_s(\mu_0)}^{\alpha_s(\mu)} \frac{d\alpha}{\beta(\alpha)}\left[\gamma_+(\alpha) + \Gamma_{\rm cusp}(\alpha)\int_{\alpha_s(\mu_0)}^{\alpha}\frac{d\alpha'}{\beta(\alpha')}\right]. \tag{B8}$$

In order to make the composition rule (8) manifest, it is convenient to introduce a reference scale, μ_*, which in the numerical analysis we identify with the hadronic input scale μ_0. To this end, we rewrite the function V as

$$\begin{aligned} V(\mu,\mu_0) &= -\int_{\alpha_s(\mu_0)}^{\alpha_s(\mu)} \frac{d\alpha}{\beta(\alpha)}\left[\gamma_+(\alpha) + \Gamma_{\rm cusp}(\alpha)\int_{\alpha_s(\mu_*)}^{\alpha}\frac{d\alpha'}{\beta(\alpha')}\right] - \int_{\alpha_s(\mu_0)}^{\alpha_s(\mu)} \frac{d\alpha}{\beta(\alpha)}\,\Gamma_{\rm cusp}(\alpha)\int_{\alpha_s(\mu_0)}^{\alpha_s(\mu_*)}\frac{d\alpha'}{\beta(\alpha')} \\ &\equiv V_*(\mu,\mu_0) - g(\mu,\mu_0)\,\ln\frac{\mu_*}{\mu_0}\,. \end{aligned} \tag{B9}$$

With this, the RG elements read

$$U_{\omega'}(\mu,\mu_0) = \exp\left[V_*(\mu,\mu_0) - g(\mu,\mu_0)\,\ln\frac{\mu_*}{\hat{\omega}'}\right], \tag{B10}$$

and, by definition,

$$V_*(\mu_2,\mu_1) + V_*(\mu_1,\mu_0) = V_*(\mu_2,\mu_0)\,, \qquad g(\mu_2,\mu_1) + g(\mu_1,\mu_0) = g(\mu_2,\mu_0)\,, \tag{B11}$$

which implies the composition rule for $U_{\omega'}$. Explicit expansions for the RG functions can now be obtained by inserting the perturbative expressions for the β-function and anomalous dimension. Using the abbreviations

$$r_0 \equiv \frac{\alpha_s(\mu_0)}{\alpha_s(\mu_*)}\,, \qquad r_1 \equiv \frac{\alpha_s(\mu_1)}{\alpha_s(\mu_*)}\,, \tag{B12}$$

we find $g(\mu_1,\mu_0)$ to 3-loop accuracy,

$$\begin{aligned} g(\mu_1,\mu_0) = {}& \frac{\Gamma_0}{2\beta_0}\,\ln\frac{r_0}{r_1} + \frac{\alpha_s(\mu_*)}{4\pi}\,\frac{\beta_0\Gamma_1 - \beta_1\Gamma_0}{2\beta_0^2}\,(r_0 - r_1) \\ & + \left(\frac{\alpha_s(\mu_*)}{4\pi}\right)^2 \frac{\beta_0^2\Gamma_2 - \beta_2\beta_0\Gamma_0 - \beta_1\beta_0\Gamma_1 + \beta_1^2\Gamma_0}{4\beta_0^3}\,(r_0^2 - r_1^2) + \ldots \end{aligned} \tag{B13}$$

Similarly, for the function $V_*(\mu_1,\mu_0)$ one gets

$$\begin{aligned} V_*(\mu_1,\mu_0) = {}& \frac{\pi}{\alpha_s(\mu_*)}\,\frac{\Gamma_0}{\beta_0^2}\left(\frac{1}{r_0} - \frac{1}{r_1} + \ln\frac{r_0}{r_1}\right) - \frac{\gamma_0}{2\beta_0}\,\ln\frac{r_0}{r_1} \\ & - \frac{\beta_0\Gamma_1 - \beta_1\Gamma_0}{4\beta_0^3}\left(r_1 - r_0 + \ln\frac{r_0}{r_1}\right) - \frac{\beta_1\Gamma_0}{8\beta_0^3}\,(\ln^2 r_0 - \ln^2 r_1) + \ldots \end{aligned} \tag{B14}$$

where we neglected terms of order α_s, as the 2-loop result for the anomalous-dimension coefficient γ_1, which will enter at that order, is currently unknown. Notice that the so constructed expansions of g and V_*, and thus the expansion of $U_{\omega'}$, respect the composition rule (which would not have been the case if one had expanded the function V directly).

[1] G. Bell, Th. Feldmann, Y.-M. Wang and M. W. Y. Yip, JHEP **1311** (2013) 191 [arXiv:1308.6114 [hep-ph], arXiv:1308.6114].

[2] B. O. Lange, M. Neubert, Phys. Rev. Lett. **91** (2003) 102001 [hep-ph/0303082].

[3] S. J. Lee, M. Neubert, Phys. Rev. D **72** (2005) 094028 [hep-ph/0509350].

[4] M. Beneke, G. Buchalla, M. Neubert and C. T. Sachrajda, Phys. Rev. Lett. **83** (1999) 1914 [hep-ph/9905312].

[5] Z. Ligeti, I. W. Stewart and F. J. Tackmann, Phys. Rev. D **78** (2008) 114014 [arXiv:0807.1926 [hep-ph]].

[6] P. Ball and A. N. Talbot, JHEP **0506** (2005) 063 [hep-ph/0502115].

[7] A. G. Grozin and M. Neubert, Phys. Rev. D **55** (1997) 272 [arXiv:hep-ph/9607366].

[8] G. Bell and T. Feldmann, JHEP **0804** (2008) 061 [arXiv:0802.2221 [hep-ph]].

[9] M. Knodlseder and N. Offen, JHEP **1110** (2011) 069 [arXiv:1105.4569 [hep-ph]].

[10] S. Descotes-Genon and N. Offen, JHEP **0905** (2009) 091 [arXiv:0903.0790 [hep-ph]].

[11] A. V. Efremov and A. V. Radyushkin, Phys. Lett. B **94** (1980) 245.

[12] G. P. Lepage and S. J. Brodsky, Phys. Lett. B **87** (1979) 359; Phys. Rev. D **22** (1980) 2157.

[13] H. Kawamura, J. Kodaira, C. -F. Qiao, K. Tanaka, Phys. Lett. B **523** (2001) 111 [Erratum-ibid. B **536** (2002) 344] [hep-ph/0109181]; H. Kawamura and K. Tanaka, Phys. Lett. B **673** (2009) 201 [arXiv:0810.5628 [hep-ph]].

[14] V. M. Braun, D. Y. Ivanov and G. P. Korchemsky, Phys. Rev. D **69** (2004) 034014 [arXiv:hep-ph/0309330].

[15] M. Beneke and J. Rohrwild, Eur. Phys. J. C **71** (2011) 1818 [arXiv:1110.3228 [hep-ph]].

[16] V. M. Braun and A. Khodjamirian, Phys. Lett. B **718** (2013) 1014 [arXiv:1210.4453 [hep-ph]].

[17] S. W. Bosch, B. O. Lange, M. Neubert and G. Paz, Phys. Rev. Lett. **93** (2004) 221801 [hep-ph/0403223].

[18] Y. Amhis *et al.* [Heavy Flavor Averaging Group Collaboration], arXiv:1207.1158 [hep-ex].

[19] G. P. Korchemsky and A. V. Radyushkin, Nucl. Phys. B **283** (1987) 342.

[20] I. A. Korchemskaya and G. P. Korchemsky, Phys. Lett. B **287** (1992) 169.

[21] S. Moch, J. A. M. Vermaseren and A. Vogt, Nucl. Phys. B **688** (2004) 101 [hep-ph/0403192].

[22] M. Neubert, Eur. Phys. J. C **40** (2005) 165 [hep-ph/0408179].

[23] V. M. Braun and A. N. Manashov, arXiv:1402.5822 [hep-ph].

[24] It has recently been shown [23] that (9) can be understood as the momentum-space representation of the eigenvectors of one of the generators of collinear conformal transformations.

[25] If the hadronic model under consideration gives an explicit reference to the renormalization scale μ_0, one would have to replace $\mu_0 \to \mu_{\omega'}(\mu_0)$ in $\rho^{\rm model}(\omega', \mu_0)$.

[26] In this work we do not entertain the idea to change the mass scheme in the perturbative matching procedure itself. Although a renormalon-free scheme like the one proposed in [3] would improve the perturbative convergence for the regularized moments M_n, we do not expect a significant effect for the logarithmic moments relevant for phenomenological applications since, as we will show below, the contributions from the perturbative regime are subdominant there.